EXPERIMENTAL CHARACTERIZATION OF AN OPERATING VESTAS V27 WIND TURBINE USING HARMONIC POWER SPECTRA AND OMA SSI

Dmitri Tcherniak[1], and Matthew S. Allen[2]

[1] Brüel & Kjær Sound and Vibration Measurement A/S, dmitri.tcherniak@bksv.com

[2] Department of Engineering Physics, University of Wisconsin-Madison, msallen@engr.wisc.edu

ABSTRACT

The study addresses experimental identification of linear periodic time variant systems. The recently introduced Harmonic-OMA-Time Domain (H-OMA-TD) method is in focus. It is shown how this method can aid engineers and what additional information it can bring, compared to other methods. The method is demonstrated in application to experimental data obtained on operating wind turbine.

Keywords: Operating Wind Turbine, Periodic Time Variant Systems, LPTV, LTP, Floquet analysis, Fourier exponents.

1. INTRODUCTION

Modern wind turbines are designed to generate energy for a period of 20 to 25 years. Exposed to enormous loads and manufactured from light materials, the wind turbine structure is subjected to strong vibrations. To ensure the turbine produces energy and stays undamaged during the intented lifespan, the design engineers need to fully understand the dynamics of operating wind turbines. This is not a trivial task. The well-accepted modal analysis approach is only applicable under a very limited set of conditions, since its main assumption is that the system of interest is linear time invariant (LTI). Wind turbines are not linear time invariant if one considers the most natural reference frame, where the vibration of the blades is measured relative to the moving rotor reference frame and the tower is measured in the fixed reference frame. In that reference frame, the system contains stiffness terms that vary periodically with time so it is termed linear time periodic (LTP) or linear periodically time varying (LPTV). However, for several decades wind turbines have been modeled as LTI by using the multi-blade coordinate (MBC, or also known as Coleman) transformation, which replaces the motion of the individual blades with rotor coordinates that describe the motion of the rotor as a whole.

The MBC transformation provides a simple and intuitive approach for treating LPTV systems. It is a special coordinate transformation, which converts the equations of motion (EoM) of a bladed, rotating structure into a time invariant system [1]. After such a transformation, the obtained LTI system can be analysed by conventional modal analysis methods. This transformation only succeeds in producing a

LTI system if the rotor is perfectly isotropic and the blades are equally spaced, i.e., all blades are structurally identical and evenly and identically attached to the hub. Effects such as blade-to-blade variations, wind shear, active-pitch control, incomplete instrumentation (in an experiment) and gravitational stiffening cannot be captured with an LTI model. This work employs a more versatile approach where the turbine is modeled as an LPTV system, which requires application of other analysis techniques. Fortunately, modal analysis extends very naturally to LPTV systems (see, e.g., [2]), so this does not complicate experiments or analysis too dramatically.

Analysis methods for time periodic systems have existed for several decades, for example the MBC, transformation, Floquet analysis and Hill's method, and they are implemented in some of the simulation software that is used for designing wind turbines and helicopters [3]. While these works often present Floquet theory in a way that seems disconnected from LTI modal analysis, one key outcome of Floquet theory is that modal decomposition is still applicable to LPTV systems but the mode shapes are periodic (the eigenvalues or poles are constant). Expanded into Fourier series, each mode will consist of infinitely many components, each oscillating at frequency equal to the modal frequency plus an integer multiple of the rotational frequency. Hence, each time-varying shape is manifested by sidebands in the spectrum. Each sideband component will also have its own shape . In this regard, when performing frequency domain analysis the primary difference between LTI and LPTV systems is that the latter has multiple deformation shapes for each eigenvalue and these must be added to obtain each mode's complete, time-periodic mode shape.

Naturally, LPTV analysis produces the same result as the MBC transformation if the rotor is isotropic. Skjoldan et al. [4] demonstrated the similarity between MBC transformation and Floquet analysis, and showed that only three harmonic components are necessary to describe each mode shape of a three-bladed isotropic rotor. If the rotor is not isotropic, then MBC breaks down and more than three harmonics will be present for some or all of the modes. Using Floquet analysis, one can show that slightly anisotropic rotors require more than three components. However, numerical simulations demonstrated that sometimes only a few components are significant and the rest can be neglected without loss of the accuracy, see for example [5].

1.1. Experimental techniques for LPTV systems analysis

Engineering practice often requires design validation after the wind turbine prototype is constructed; this calls for *experimental* system identification. The tools allowing experimental dynamic characterization of LPTV systems are very limited: one can name MBC transformation adapted to experimental identification [6], the extension of SSI to LPTV systems based on angular resampling [7] and harmonic power spectra (HPS) method [2]. All these methods are output-only, i.e., they do not require measurement of the input to the system. Instead, they assume that the input forces excite all system modes, have broadband spectra and are uncorrelated.

1.1.1. Multiblade Coordinate Transformation (MBC)

The adaptation of the MBC transformation method to experimental modal analysis starts with pre-processing of the experimental data, namely, the conversion of the coordinates q measured in the rotating frame to the ground-fixed multi-blade coordinates a_0, a_1, b_1:

$$a_{0,k} = \frac{1}{3}\sum_{i=1}^{3} q_{i,k}, \qquad a_{1,k} = \frac{2}{3}\sum_{i=1}^{3} q_{i,k}\cos(\phi_i), \qquad b_{1,k} = \frac{2}{3}\sum_{i=1}^{3} q_{i,k}\sin(\phi_i), \tag{1}$$

where $i = 1, 2, 3$ is the blade index, k is the index of the DOF and ϕ_i is the azimuth of the ith blade. After that, conventional OMA (for example, the SSI technique) is applied. The obtained modal parameters are then transferred back into the rotating using the backward MBC transformation:

$$q_{i,k} = a_{0,k} + a_{1,k}\cos(\phi_i) + b_{1,k}\sin(\phi_i). \tag{2}$$

The overall process is shown schematically in Figure 1. The examples of this technique in application to operating wind turbine data can be found in [6], **Error! Reference source not found.**-[10].
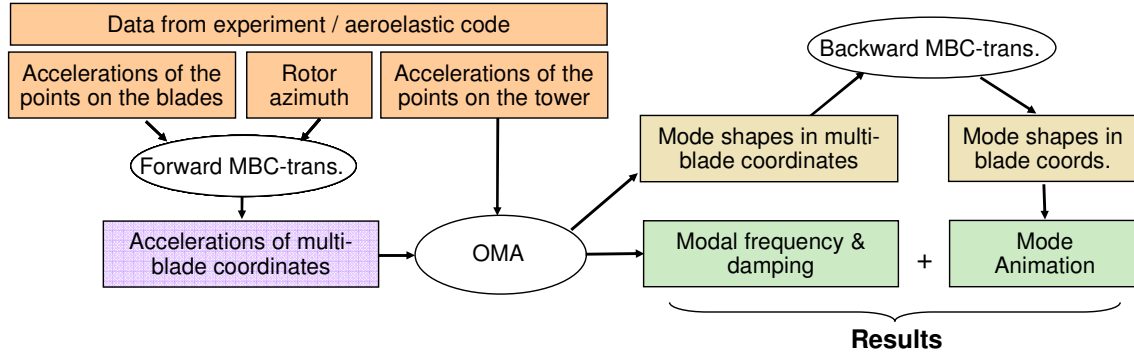
Figure 1. Adaptation of the MBC transformation method to experimental modal analysis (from [6]).

Assuming constant rotor speed Ω [thus the azimuth $\phi_i = \Omega t + \frac{2\pi}{3}(i-1)$], it can be easily shown that the mode shape of the rth mode in the rotating frame is [1], [9]:

$$q_{i,k}(t) = A_{0,k}\sin(\omega_r t + \varphi_0) + A_{BW,k}\sin\left((\omega_r + \Omega)t + \frac{2\pi}{3}(i-1) + \varphi_{BW}\right) + \\ A_{FW,k}\sin((\omega_r - \Omega)t - \frac{2\pi}{3}(i-1) + \varphi_{FW}),$$ (3)

where ω_r is the natural frequency of the rth mode. The modal amplitudes and phases in (3) can be readily calculated from the corresponding eigenvector of the system in multi-blade coordinates. Analyzing (3), one can note that:

1. The mode shape is time-periodic.
2. It consists of three components.
3. The three components oscillate at frequencies ω_r, $\omega_r + \Omega$ and $\omega_r - \Omega$, respectively.
4. All three blades have the same oscillation magnitudes.
5. The phase between the blades is 0 for the first component (thus it is called *collective* component), -120^0 for the second (*backward whirling* component) and $+120^0$ for the third (*forward whirling* component).

As mentioned before, the MBC transformation assumes rotor isotropy. In reality, all rotors have some degree of anisotropy, which manifests itself in richer dynamics: one observes more components (sidebands) and the component shapes loose the regularity (equal blades' magnitude and $0/\pm 120^0$ phase) [11], [12]. As demonstrated above, MBC transformation is not capable of catching these phenomena, and consequently, application of MBC to anisotropic rotors may lead to erroneous results. This was observed, for example, in [10]. Furthermore, when dealing with measurements, the MBC requires the "isotropy" of the sensor setup: the sensors should be located at identical points on all blades and have the same orientation of measurement axis. Furthermore, if one sensor fails, then all sensors at that radial position must be discarded.

1.1.2. Lifting method

Jhinaoui et al. [7] suggested a subspace identification method specially developed for rotating systems. The method identifies the underlying Floquet eigenstructure of the rotating system and uses the special resampling procedure known as lifting ([13], [14], [15]), where the samples are obtained at the same position of the rotor at the consecutive revolutions. The drawback of the method is that it may crowd the frequency spectrum since the resampling procedure essentially aliases the signal, and it may require data from many rotor revolutions. The method showed good results for helicopter rotors, where the rotation speed is relatively high and allows thousands of rotor revolutions when the other parameters do not change. In the case of wind turbines, with their low rotation speeds, it is difficult to collect the data from several thousand rotor revolutions under the same environmental conditions (e.g., wind speed and direction) [16].

1.1.3. HPS method in frequency domain: H-OMA-FD

The rigorous proof and description of the HPS method can be found in [17]. The method is based on the concept of harmonic transfer functions [17], which were written in terms of a modal decomposition and used to develop a framework for operational modal analysis in [18]. The core of the method is the modulation of the response signals using the phasors rotating with the fundamental circular frequency Ω and its integer multipliers:

$$\mathbf{y}_m(t) = \mathbf{y}(t)e^{-jm\Omega t},\tag{4}$$

where $\mathbf{y}(t)$ is a vector of N measured responses and m is an integer varying from $-M$ to M. The resulting vector consists of $N(2M + 1)$ complex time histories.

The next step of the method is the calculation of the harmonic power spectra (HPS) matrix between the modulated signals; this is done in the same manner as in the LTI case:

$$\mathbf{S}_{YY}(\omega) = \mathrm{E}\langle \mathbf{y}_m(\omega)\mathbf{y}_m(\omega)^H \rangle,\tag{5}$$

where $\mathrm{E}\langle...\rangle$ is mathematical expectation, $(...)^H$ is Hermetian transpose. Note that the resulting matrix is defined in the frequency domain. The theory in [18] shows that the HPS matrix can be presented in terms of modes of the LPTV system. Preserving only dominant terms, one can prove that the following is valid:

$$\mathbf{S}_{YY}(\omega) \approx \sum_{r=1}^{2K} \sum_{l=-\infty}^{\infty} \frac{\mathbf{c}_{r,l}\mathbf{W}(\omega)\mathbf{c}_{r,l}^H}{(j\omega - (\lambda_r - jl\Omega))(j\omega - (\lambda_r - jl\Omega))^H}\tag{6}$$

where λ_r are the Floquet exponents, $\mathbf{c}_{r,l}$ are the Fourier coefficients that describe the temporal and spatial deformation pattern of the periodic mode shape, and K is the number of modes. $\mathbf{W}(\omega)$ describes the input spectrum. Under the standard OMA assumptions regarding the excitation, namely that the input is uncorrelated random white noise, $\mathbf{W}(\omega)$ becomes constant.

The last task is to extract the Floquet exponents and Fourier coefficients from the HPS matrix. This can readily be done by employing one of the conventional frequency domain methods, for example, AMI [19] or more sophisticated AFPoly algorithm [20] or pLSCF [21].

1.1.4. H-OMA-TD: combination of HPS and OMA SSI

In operational modal analysis, the time domain techniques are sometimes more advantageous than the frequency domain ones, especially in the case of heavily damped structures, which is typical for operating wind turbines. The extension of HPS to the time domain was suggested and explained in [12]. We referred this extension as Harmonic OMA Time Domain (H-OMA-TD), to distinguish it from the frequency domain HPS method (H-OMA-FD). In that study, the method was applied to an analytical system: a six-degrees-of-freedom system representing a three-bladed rotor with blades that were flexible only in in-plane direction. The availability of the EoM allowed the application of Floquet analysis to obtain the analytical periodic modes. The analytical solution served as a reference for validation of the experimental identification. The response of the rotor to random loads was simulated and the resulting response time histories were used as an input to H-OMA-TD. The comparison with the analytical solution showed quite good agreement. The method was capable of catching the features of the anisotropic rotor dynamics, both qualitatively and quantitatively.

The presented study demonstrates the application of the method to data measured on a real object: an operating Vestas V27 wind turbine.

2. INTRODUCTION TO H-OMA-TD

The flow of H-OMA-TD is schematically shown in Figure 2. The measured responses (on the rotating and non-rotating parts of the structure) form vector $\mathbf{y}(t)$. The rotational speed or, preferably, the rotor azimuth should be measured as well. The first step is the same as in H-OMA-FD, namely the modulation (4). The resulting time histories are complex (except the original time histories, which correspond to $m = 0$). Since the standard implementation of the OMA SSI algorithm can only accept real-valued time histories, a conversion is required. The conversion shall, however, retain the magnitude and phase relations between the original signals and their modulated copies. The method suggested in [12] takes the following steps:

1. For the exponentially modulated signals $\mathbf{y}_m(t)$, compute their periodogram $\mathcal{F}(\mathbf{y}_m(t))$ using a fast Fourier transform. The periodogram of complex $\mathbf{y}_m(t)$ is not a Hermitian function, i.e., its negative frequency part is not a complex conjugate of the positive frequency part.
2. Replace the negative frequency part of the periodogram by the complex conjugate of the positive part.
3. Using inverse FFT, generate the new time signals $\tilde{\mathbf{y}}_m(t)$, which are real.
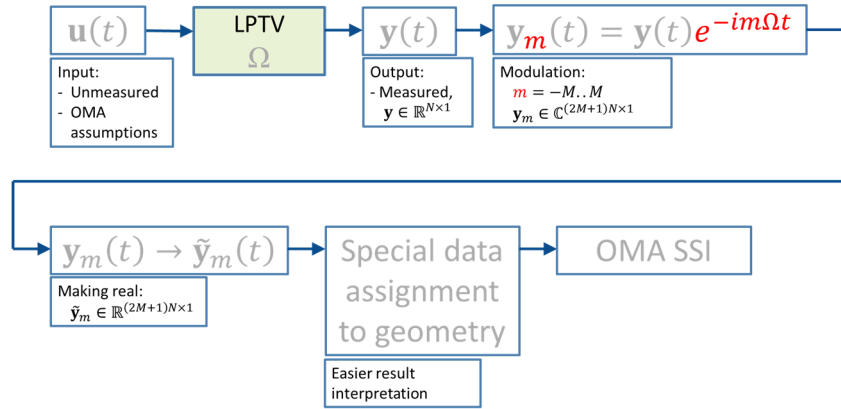

Figure 2. H-OMA-TD flow chart.

The next step, the *special data assignment to geometry*, is mainly to facilitate the mode visualization: indeed, the periodic mode shape is not easy to interpret; instead, we propose to visualize the component shapes.

Following the proposed approach, one has to create $2M$ "clones" of the geometry, for example, right and left from the original geometry, Figure 3. The mth "clone" will visualize the mth component. The data assignment shall be conducted accordingly: the time histories modulated with the given m shall be assigned to the mth clone.
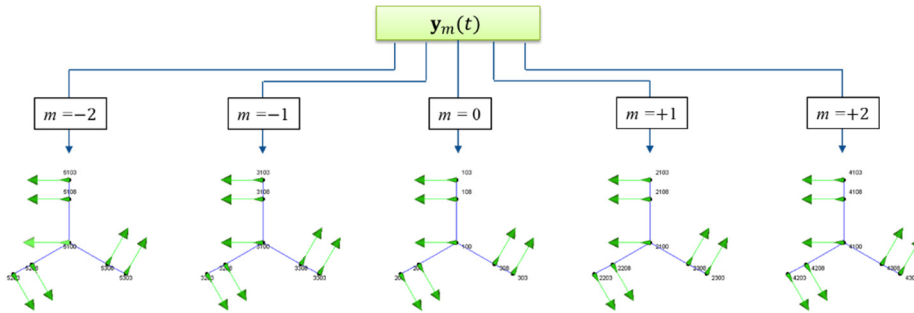

Figure 3. Assignment of the modulated signals to geometry.

3. VIBRATION MEASUREMENTS ON OPERATING VESTAS V27

A detailed description of the instrumentation and data acquisition was presented in [22]; this section provides a brief overview.

Vestas V27 is a 225kW pitch-controlled horizontal-axis wind turbine with 27 m rotor diameter (blade length is 13 m). The wind turbine is not new but has many features similar to those of modern wind turbines (Figure 4).

Each of the three blades of the wind turbine was instrumented by 12 monoaxial accelerometers, ten measuring in the flap- and two in the edgewise direction. Since the MBC transformation was considered as the main analysis tool, special care was taken to instrument all three blades as identically as possible in regard to both the accelerometers' location and orientation. Also, the pitch angle and rotor azimuth were measured using dedicated sensors. The data was collected by a data acquisition front end located in the spinner and wirelessly transmitted the data to the nacelle. The front end was powered via a slip ring.

The nacelle vibrations were measured by three triaxial accelerometers, one located under the main bearing and the other two at the rear of the nacelle; a laser tacho probe was used to measure the rotational speed of the high-speed shaft. To sample-synchronize the rotor and nacelle data streams, the IRIG-B GPS-based protocol was employed.

Figure 4. Vestas V27 wind turbine. The green strips on the blades are the tape protecting the accelerometer cables.

The measurement campaign started in October 2012 and ended in May 2013, thus covering a wide range of weather conditions and wind speeds. We recorded data during the entire campaign, except for short periods when the system was down. During the campaign, a few accelerometers were lost (it was discovered later that this was due to improper cabling). Using a data management system, it was straightforward to find recordings where the wind speed, RPM and pitch angle were not changing significantly, and these recordings were selected for the following analysis.

The data from this measurement campaign was already analysed and presented: In [9], the MBC and H-OMA-FD approaches were used for edgewise rotor modes. In [10], the MBC transformation was employed for both flap- and edgewise modes. In [16], the edgewise rotor modes were analysed using the lifting approach.

4. PROCEDURE AND RESULTS

The blade vibrations are caused by various loads. The wind-induced aerodynamic forces are the main contributor. Though intuitively these forces should satisfy OMA assumptions, the aerodynamic analysis shows that this is not true. The aerodynamic forces do not have flat frequency spectra; they are rather characterized by peaks at the rotation frequency and its harmonics with thick tails around each peak. More details can be found in [23]. Slight rotor unbalancing and aerodynamic interaction with the tower also cause some periodicity in the measured signals. In addition to this, the high-speed-shaft-related vibrations propagate through the low-speed shaft and, being sampled by the rotor frequency, appear as a series of sharp peaks at the higher frequencies separated by the rotor frequency (Figure 5).

An OMA algorithm may confuse the sharp peaks with the system modes. Therefore, it is advantageous to remove the deterministic component from the measured responses by dedicated methods (see. e.g.. [24] for an overview). Since both rotor azimuth angle and the high-speed-shaft RPM measurements were available, we selected the Time Synchronous Averaging (TSA) method to remove the deterministic part from the response signals. The spectra from the edgewise tip accelerometer before and after TSA are shown in Figure 5 as an example.
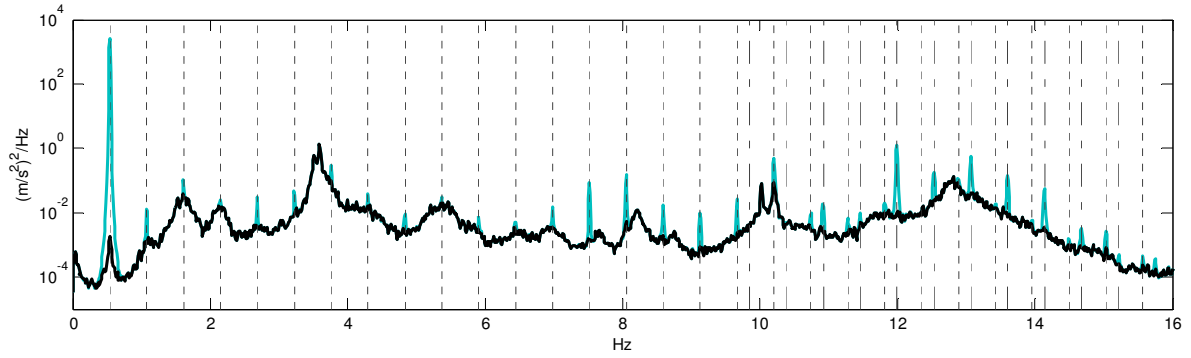
Figure 5. Power spectral density of the edgewise tip accelerometer of blade #2, before (green) and after (black) TSA. The dashed lines are rotor harmonics, dash-dot lines – high-speed-shaft-related harmonics.

An operating wind turbine has rich dynamics and variety of modes. However, the objective of the paper is not to describe V27's dynamics. It is rather to demonstrate the H-OMA-TD method and show how it can aid engineers, and what additional information it can bring, compared to other methods.

To demonstrate the method, we selected the in-plane rotor modes (which correspond to the edgewise blade motion). In total, seven signals were used: the edgewise accelerometer signals from each blade's tip and at 2/3 of the blade length, denoted $q_{i,tip}$ and $q_{i,mid}$, respectively, and the front nacelle acceleration in the side-to-side direction, x_N. Thus the vector $\mathbf{y}(t)$ in (4) is:

$$\mathbf{y}(t) = \left\{ x_N(t), q_{1,tip}(t), q_{1,mid}(t), q_{2,tip}(t), q_{2,mid}(t), q_{3,tip}(t), q_{3,mid}(t) \right\}^T . \tag{7}$$

Twenty-minute-long recordings corresponding to 32 RPM and 43 RPM regimes were analyzed. The results presented below are for 32 RPM. The signals were pre-processed by TSA and then modulated with $M = 2$. Since the RPM was not exactly constant during the recordings, we used the measured azimuth $\phi_1(t)$ instead of Ωt in (4).

4.1. Whirling modes

The two first edgewise rotor modes are dominated by the whirling components, Figure 6; the magnitude of their closest sidebands is at least a decade less. The dominant components occur at 3.52Hz (forward whirling mode) and 3.59Hz (backward whirling mode), – the modes are named after their dominant component. The damping of these two modes is 0.5% and 0.8%, respectively. The shapes of the obtained components are similar to those obtained using the H-OMA-FD method; see Figure 11 in [9].

The magnitudes of the three blades are different and the phase lag between them is not $\pm 120^0$, as one would expect for the isotropic rotor. As we mentioned before, the MBC transformation cannot capture these features of the rotor dynamics. The idea of employing the magnitude and phase irregularity as an indicator of rotor anisotropy due to damage or ice formation was examined in [25].

The above-mentioned shape irregularity leads to erroneous and confusing results, which can be observed when applying the MBC transformation to anisotropic rotors: for example, the method finds four modes instead of two, see Figure 7a in [10].

Observing such a low magnitude of the sidebands, one may suggest that using dedicated LPTV methods for three-bladed rotors is not necessary and it only results in over complication of the analysis. Indeed, by setting $M = 0$, meaning that we simply applying OMA to the raw measured data, one will end up with almost the same results. This, however, is only relevant for these two particular modes, and the following examples will demonstrate much more complex dynamics of other modes, where the H-OMA-TD method has obvious advantages. Furthermore, a sideband with an amplitude that is an order of magnitude smaller than expected can still produce a significant error for certain harmonic *inputs*. The variation of the mode shapes in time might also lead to instability at other rotor speeds even though the sidebands are small at this speed.
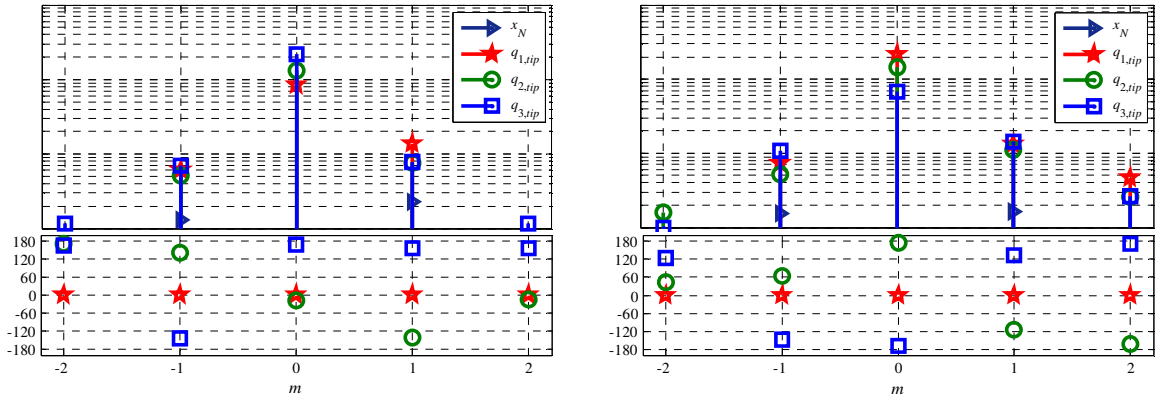
Figure 6. Shapes of the components of the forward whirling mode (left) and backward whirling mode (right): magnitudes and phases.

4.2. Collective mode

The dynamics of the first rotor collective mode are more interesting: though the collective component at 8.22Hz is dominant, the magnitude of the right and left sideband components is only about five times smaller (Figure 7). The damping of this mode is 1%.The component corresponding to the left sideband ($m = -1$) at 7.69Hz constitutes the forward whirling, and the right sideband ($m = 1$) at 8.76Hz is backward whirling; this can be seen from the phase lag between the blades. The central ($m = 0$) collective component has a significant tower part. Interesting to note, the collective mode is seemingly unaffected by the rotor anisotropy, whose effect was clearly seen in the whirling modes: here the blade magnitudes are almost equal and the phase lag between the blades is 0 for the collective component and $\pm 120^0$ for the whirling components. The magnitudes of the components corresponding to $m = \pm 2$ are 10 to 20 times smaller than the dominant one.

Since the rotor anisotropy does not play a significant role in the dynamics of this mode, the MBC transformation can be employed and will lead to the similar results: all three dominant components will be well identified. However, the proposed H-OMA-TD approach readily allows the visualization of the components, without involving any backward coordinate transformation.
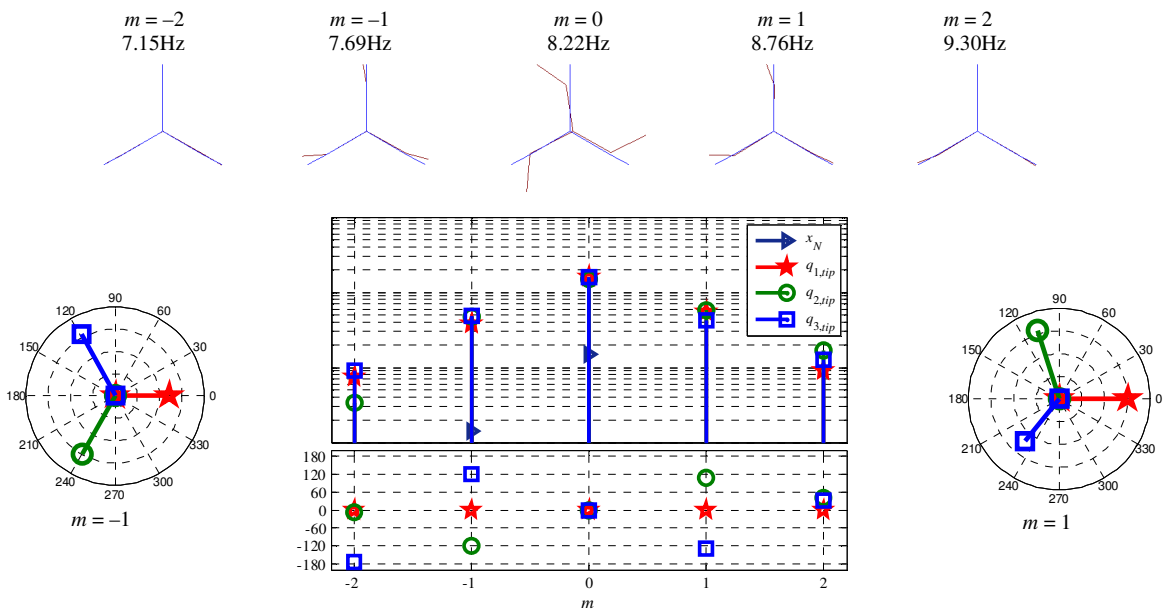

Figure 7. Shapes of the components of the collective mode. Top: visualization; bottom: magnitudes and phases. Sides: complexity plots of the whirling components.

4.3. Tower mode

The first side-to-side tower mode is observed at approximately 1Hz with damping 1.8%. This agrees well with the simulations and modal analysis performed on the nacelle data only [10]. However, utilizing the accelerometers mounted on the blades one can see that the expected side-to-side tower bending has a strong effect on the rotor. This declares itself as a strong collective rotor component at 1.54Hz ($m = 1$) and whirling component at 2.08Hz ($m = 2$), as shown in Figure 8. Actually, the dominant tower motion at 1.00Hz ($m = 0$) is also accompanied by the whirling rotor motion. It is important to note how easy it was to consider the tower and blade motions together using time-periodic H-OMA theory; these measurements would be more difficult to interpret without it.

Unfortunately, we cannot say anything certain for the components at $m = -1$, -2: the triaxial accelerometers used for the nacelle instrumentation had a high background noise level at frequencies below 0.7Hz, making the observations at these frequencies unreliable.
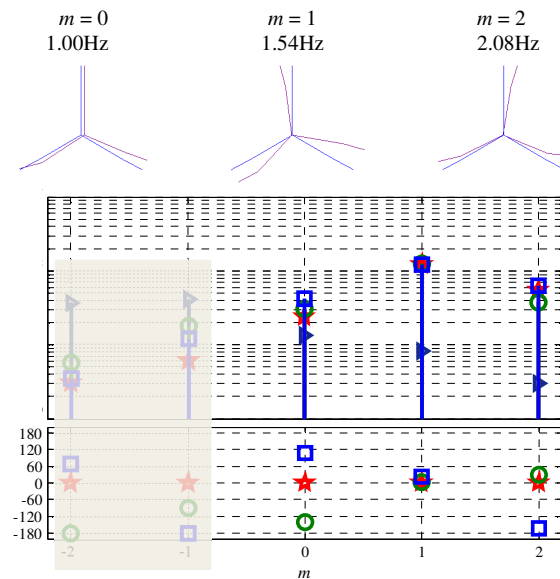

Figure 8. Shapes of the components of the first side-to-side tower mode. Top: visualization; bottom: magnitudes and phases. The components at $m = -1$, -2 are not reliable due to accelerometer noise, thus they are dimmed.

4.4. General observations

Examining the four modes, one cannot come to a clear guidance on how many modal components should be taken into consideration, i.e., which M to choose in Eq. (4). Both whirling modes are dominated by a single component, thus $M = 0$ might be sufficient; the collective mode has three significant components, thus M should be chosen greater than one. The tower mode perhaps require even more components. According to the theory behind MBC transformation, three components (i.e.. $M = 1$) are sufficient to describe the dynamics of isotropic rotor in the absence of gravity. However, the gravity and slight rotor anisotropy may require more components. Increasing M, one automatically increases the number of signals $\mathbf{y}_m$ and hence, the complexity of the analysis. From authors' opinion, for three-bladed rotors with possible slight anisotropy, $M = 2$ is a reasonable choice. However, one needs to be careful applying this to, e.g., two-bladed rotors, where the periodic behaviour is much stronger. Also, if one is interested in behaviour that occurs over a small fraction of the cycle, say due to the blades passing the tower, then one might need many more harmonics.

5. CONCLUSION

The paper compares the recently suggested H-OMA-TD method with other methods intended to deal with time-periodic dynamic systems and demonstrates the method by application to experimentally obtained data from an operating wind turbine. It is shown that the method has a number of advantages:

1. It does not require rotor isotropy.
2. It allows using robust time domain OMA algorithms, such as OMA SSI:
   - It does not require any modification of OMA algorithms: a standard commercial implementations can be used
3. It correctly scales the magnitudes of the components with respect to each other, though the entire mode shape is normalized, as it is typical for OMA.
4. It does not require the data from many rotor revolutions for robust system identification.
5. It proposes the visualization scheme, which enables an easy interpretation of the periodic modes.

The method still misses a rigorous mathematical proof; so far, it is very much built on the analogy with H-OMA-FD method.

ACKNOWLEDGEMENTS

REFERENCES

[1]   Hansen, M.H. (2003) Improved Modal Dynamics of Wind Turbines to Avoid Stall-induced Vibrations. *Wind Energy*, 6, 179-195.

[2]   Allen, M. S. (2009) Frequency-Domain Identification of Linear Time-Periodic Systems using LTI Techniques, *Journal of Computational and Nonlinear Dynamics*, 4(24).

[3]   Peters, D. A. (1994) Fast Floquet theory and trim for multi-bladed rotorcraft, *Journal of the American Helicopter Society*, 39, 82-89.

[4]   Skjoldan, P. F., Hansen, M. H. (2009) On the similarity of the Coleman and Lyapunov-Floquet Transformations for Modal Analysis of Bladed Rotor Structures, *Journal of Sound and Vibration*, 327, 424-439.

[5]   Skjoldan, P.F. (2011) Aeroelastic Modal Dynamics of Wind Turbines Including Anisotropic Effects. *PhD Dissertation.* Risø, Technical University of Denmark, Denmark.

[6]   Tcherniak, D., Chauhan, S., Rossetti, M., Font, I., Basurko, J., Salgado, O. (2010) Output-only Modal Analysis on Operating Wind Turbines: Application to Simulated Data. *Proc. of European Wind Energy Conference*, Warsaw, Poland.

[7]   Jhinaoui, A., Mevel, L., Morlier, J. (2014) A new SSI algorithm for LPTV systems: application to a hinged-bladed helicopter. *Mechanical Systems and Signal Processing*, 42(1), 152–166.

[8]   Di Lorenzo, E., Manzato, S., Peeters, B., Marulo F. (2014) Structural health monitoring techniques applied to operating wind turbines, *Proc. of the 9th Int. Conference on Structural Dynamics, (EURODYN 2014)*, Porto, Portugal.

[9]   Yang, S., Tcherniak, D., Allen, M. S. (2014) Modal Analysis of Rotating Wind Turbine using Multi-blade Coordinate Transformation and Harmonic Power Spectrum, *Proc. 32nd Int. Modal Analysis Conference (IMAC XXXII)*, Orlando, FL, USA.

[10] Requesón, O.R., Tcherniak, D., Larsen, G.C. (2015) Comparative Study of OMA Applied to Experimental and Simulated Data from on Operating Vestas V27 Wind Turbine, *Proc. Int. Operational Modal Analysis Conference (6th IOMAC)*, Gijón, Spain.

[11] Skjoldan, P.F. (2009) Modal Dynamics of Wind Turbines with Anisotropic Effects. *Proc. of 47th AIAA Aerospace Sciences Meeting*. Orlando, FL, USA.

[12] Tcherniak, D., Yang, S., Allen, M.S. (2014) Experimental characterization of operating bladed rotor using harmonic power spectra and stochastic subspace identification. *Proc. International Conference on Noise and Vibration Engineering (ISMA)*, Leuven, Belgium.

[13] Luxemburg, L. A. (1990) Frequency analysis of time-varying periodic linear systems by using modulo p transforms and its applications to the computer-aided analysis of switched networks, *Circuits, Systems, and Signal Processing*, 9, 3-29.

[14] Yang, S., Allen, M. S. (2014) Lifting to Simplify Output-only Continuous Scan Laser Vibrometry, *Mechanical Systems and Signal Processing*, 45, 267–282.

[15] Allen, M. S., Sracic, M. W. (2010) A New Method for Processing Impact Excited Continuous-Scan Laser Doppler Vibrometer Measurements, *Mechanical Systems and Signal Processing*, 24, 721–735.

[16] Mevel, L., Gueguen, I., Tcherniak, D. (2014) LPTV Subspace Analysis of Wind Turbine Data, *Proc. European Workshop on Structural Health Monitoring (EWSHM)*, Nantes, France.

[17] Wereley, N. M. (1991) Analysis and Control of Linear Periodically Time Varying Systems. *PhD Thesis*, Department of Aeronautics and Astronautics, Massachusetts Institute of Technology, Cambridge.

[18] Allen, M. S., Sracic, M. W., Chauhan, S., Hansen, M. H. (2011) Output-Only Modal Analysis of Linear Time Periodic Systems with Application to Wind Turbine Simulation Data, *Mechanical Systems and Signal Processing*, 25, 1174-1191.

[19] Allen, M.S. (2005) Global and Multi-Input-Multi-Output (MIMO) Extensions of the Algorithm of Mode Isolation (AMI), *Doctorate thesis*, George W. Woodruff School of Mechanical Engineering, Georgia Institute of Technology, Atlanta, Georgia.

[20] Vold, H., Napolitano, K. (2007) Aliasing in modal parameter estimation: An historical look and new innovations. *Proc. of International Modal Analysis Conference (IMAC XXV)*. Orlando, FL, USA.

[21] Guillaume, P. P., Verboven, P. (2003) A Poly-Reference Implementation of the Least-Squares Complex Frequency-Domain Estimator. *Proc. of International Modal Analysis Conference (IMAC XXI)*, Kissimmee, FL, USA.

[22] Tcherniak, D., Larsen G.C. (2013) Application of OMA to an Operating Wind Turbine: Now Including Vibration Data from the Blades. *Proc. Int. Operational Modal Analysis Conference (5th IOMAC)*, Guimarães, Spain.

[23] Tcherniak, D., Chauhan, S., Hansen, M. N. (2010) Applicability Limits of Operational Modal Analysis to Operational Wind Turbines. *Proc. of Int. Modal Analysis Conference (IMAC XXVIII)*, Orlando, FL, USA.

[24] Jacob, T., Tcherniak, D., Castiglione, R. (2014) Harmonic Removal as a Pre-processing Step for Operational Modal Analysis: Application to Operating Gearbox Data. *Proc. of VDI-Fachtagung Schwingungen von Windenergieanlagen*, Bremen, Germany.

[25] Tcherniak, D. (2014) Loss of Rotor Isotropy as a Blade Damage Indicator for Wind Turbine Structural Health Monitoring Systems. *Proc. European Workshop on Structural Health Monitoring (EWSHM)*, Nantes, France.